In situ Transmission Electron Microscopy Observation of the Decomposition of MgH_2 Nanofiber

Chunyu ZHU,[a] Norihito SAKAGUCHI,[a] Sou HOSOKAI,[a] Seiichi WATANABE,[a] Tomohiro AKIYAMA[a]*

[a]Center for Advanced Research of Energy Conversion Materials, Hokkaido University, Sapporo 060-8628, Japan

*Corresponding author: Tel.: +81-11-706-6842; Fax: +81-11-726-0731.

E-mail address: takiyama@eng.hokudai.ac.jp (Tomohiro Akiyama)

ABSTRACT:

In this paper, we presented an investigation of the phase transformation of MgH_2 to Mg, in which a sample of a single-crystal MgH_2 nanofiber was prepared by hydriding chemical vapor deposition (HCVD) and observed by in situ (high-resolution) transmission electron microscopy (TEM). The results indicated that the orientation relationship between MgH_2 and Mg during the phase change was: one of the zone axis of MgH_2 <110> parallel to Mg [0001] zone axis, or one of the plane {110} of MgH_2 parallel to the basal plane of Mg (0001). On the basis of the obtained results, we proposed a structural model for the phase change of MgH_2 to Mg.

Keywords: Hydrogen storage, Magnesium hydride, nanofiber, hydriding chemical vapor deposition, TEM

1. INTRODUCTION

Magnesium is a promising candidate for solid hydrogen storage owing to its abundance, low cost, reversibility, high gravimetric H_2 density of 7.6 mass %, and high volumetric H_2 density of 110 g/L hydrogen density. However, magnesium, or magnesium hydride, has limited its practical applications because of the high operation temperature and the slow hydrogen adsorption kinetics. [1, 2] To overcome these drawbacks, most studies focus on the preparation of Mg-rich alloys and composites. [3, 4] However, this causes lowering the H_2 storage capacity due to the added weight of the elements or compounds. Another solution is to reduce the size of the Mg/Mg-based materials to the nano-scale. In order to manufacture micro/nano-structured Mg or MgH_2 and their composites many processes, such as high-energy ball milling of MgH_2 or MgH_2-based composites [3-5], magnetron sputtering for Mg thin films, [6] physical vapor-transport deposition (PVD) of Mg nanowires, [7] and hydriding chemical vapor deposition (HCVD) of MgH_2 nanofibers, [8-10] have been used. The as-prepared Mg nanowires by the PVD method having diameters ranging from 30 to 170 nm exhibit enhanced hydrogen adsorption kinetics. Most significantly, the dissociation energy for the transformation of MgH_2 to Mg and H_2 decreases drastically from 74 kJ/mol-H_2 for bulk to 65.3 kJ/mol-H_2 for nanowires with diameters of 30–50 nm.[7]

The HCVD method can be used to manufacture highly pure single-crystal nanofibers of MgH_2 on the nano/micro-scale. It has been reported that the as-prepared MgH_2 nanofibers exhibit excellent H_2 adsorption properties. [11] However, the mechanism underlying the dehydrogenation of the MgH_2 nanofibers are still not understood completely. Therefore, the purpose of this study is to observe the phase change of MgH_2 nanofiber prepared by HCVD to Mg via in situ (high-resolution) TEM, in which a structural model for elucidating the phase transformation of MgH_2 to Mg during the dehydrogenation is proposed.

2. EXPERIMENTAL

MgH_2 nanofibers were prepared by a gas-gas reaction ($H_2(g) + Mg(g) \rightarrow MgH_2(s)$), i.e. the HCVD method, as described elsewhere. [8, 9, 11] 10 g of commercially available Mg powder (purity: 99%; particle size: < 75 μm) was placed in an Inconel tube and heated to vaporize in an H_2 atmosphere (purity: 99.99999%) at 4.0 MPa and at a temperature of 600 ºC for 20 hours. The reactants, namely, the H_2 and Mg in vapor form, were deposited on the cooled Inconel flange substrate of the reactor at a temperature of 400 ~ 500 ºC to form MgH_2 nanofibers. Due to the sensitivity of MgH_2 to a moisture atmosphere, the as-prepared samples were stored in a dry Argon atmosphere.

The decomposition of MgH_2 nanofibers was induced by an electron beam, and the phase transformation of MgH_2 to Mg was observed by in-situ (high-resolution) transmission electron microscopy ((HR)-TEM, 200 kV, JEM-2010). A low-density electron beam was used to investigate the hydride and a high-density electron beam was used to decompose the hydride. A series of TEM bright-field (BF) images and selected area electron diffractions (SAEDs), before, during, and after decomposition, were obtained at the same area of an MgH_2 nanofiber. The observation for one nanofiber was completely in approximately ten minutes, and the MgH_2 nanofiber decomposed very quickly when it was irradiated with a high-density electron beam.

The MgH_2 samples were dispersed on carbon-collodion-coated copper grids in a vial by shaking it vigorously for TEM observation. The HR-TEM images were analyzed using the software Digital Micrograph (Gatan, Inc.). All the crystal structures were drawn using Crystal Studio (Version 4.0, Crystal System Co. Ltd.).

3. RESULTS AND DISCUSSION

3.1 Crystal structures of Mg and MgH_2

Magnesium has a hexagonal-close-packed (hcp) structure (space group of $P6_3/mmc$) with lattice parameters of a = b = 3.21 Å and c = 5.21 Å. [12] On the other hand, magnesium hydride has a tetragonal rutile ($P4_2/mnm$) structure with a = b = 4.50 Å and c = 3.01 Å. Figure 1 shows the unit cell images of MgH_2 and Mg. Insets of Figure 1 show the atomic arrangement for MgH_2 (110) and Mg (0001), respectively.

3.2 TEM decomposition of the MgH_2 nanofiber

Figure 2 shows a sequence of images (a, c, and e) and the corresponding SAED patterns (b, d and f) of an MgH_2 nanofiber at different stages of decomposition induced by a TEM electron beam. Image (a) and SAED pattern (b) clearly show that before decomposition, the nanofiber has a single phase, namely, that of tetragonal rutile MgH_2, as seen from the [110] zone axis. Image (c) and SAED pattern (d) show both the phases, namely, an MgH_2 phase and an Mg phase. After being exposed to a high-density electron beam, the MgH_2 nanofiber decomposed to Mg with a greater speed. Image (e) shows the completely dehydrogenated MgH_2 nanofiber and the SAED pattern (f) indicate the hexagonal Mg with [0001] zone. Images (g) and (h) show a high-resolution TEM image of Mg and a simulated lattice image obtained from the digital diffractogram as shown in (g), respectively. This lattice image of (h) indicates Mg planes of {10-10}.

Here, we index the MgH_2 SAED pattern from the [110] zone axis, as shown in Figure 2 (b), for discussing the orientation relationship of MgH_2 with Mg. It is also reasonable to index it as the [-110], [1-10] or [-1-10] zone axis, since these axes are in the same general direction of <110> having the same properties in each direction. For the hexagonal diffraction pattern of Mg from the [0001] zone axis, one can freely change the order of the face indices at the six vertices since they are on the same general face of {10-10}, and one example is shown in Figure 2 (f). It should be noted that different

indexing methods lead to different expressions for the orientation relationship between MgH_2 and Mg. Thus, we were careful during the comparison of the obtained results with those from other studies. Here, we conclude that the relationship is: one of the zone axis of MgH_2 <110> parallel to Mg [0001] zone axis, or one of the plane {110} of MgH_2 parallel to the basal plane of Mg (0001).

Figure 3 shows the results of the careful observation of the orientation relationship via the high-resolution TEM technique. Figure 3 (a) is a typical TEM image of an MgH_2 nanofiber which is partially decomposed, and Figures 3 (b) and (c) show the corresponding SAED pattern indicating both the phases of MgH_2 and Mg; this diffraction pattern is the same as that in Figure 2 (d). Figure 3 (d) is the HRTEM image of the same fiber of Figure 3 (a). Figure 3 (e) is the digital diffractogram based on Fast Fourier Transform (FFT) from the selected dash line area in (d), which shows the two phases of MgH_2 and Mg. Figures 3 (f) and (g) are the simulated diffraction pattern and lattice image of the both phases of MgH_2 and Mg based on the digital diffractogram of Figure 3 (e). By masking the diffraction spots of the MgH_2 phase, the simulated diffraction pattern of Mg [0001] and lattice image were shown in Figures 3 (h) and (i). Conversely, by masking that of Mg phase, the simulated diffraction pattern of MgH_2 [110] and lattice image were presented in Figures 3 (j) and (k).

Table 1 summarizes the results of previous studies together with those of this study. Paik B. et al. [13] observed the phase change of MgH_2 to Mg by using commercial MgH_2 powder in TEM. They obtained a series of diffraction patterns of MgH_2, which were subsequently transformed to those of Mg under irradiation by an electron beam, and summarized the relationship as MgH_2[001] // Mg[-2110] and MgH_2(-110) // Mg(0001). Bokhonov B. et al. [14] observed the orientation relationship of MgH_2 (110) parallel to Mg (0001) by using single crystals of MgH_2 whiskers. These results are the same as this study with the basal plane of Mg (0001) is parallel to one of the plane {110} for MgH_2. Schober T. [15] prepared a thin Mg disc and then hydrogenated it for TEM observation. He summarized the relationship as MgH_2(100) // Mg(0001) and MgH_2[001] // Mg[-1-120], which is different from this study. Kelekar et al. [16] reported various orientation relationships between MgH_2 and Mg according to an XRD analysis, in which epitaxial Mg thin films were deposited on different substrates and were then hydrogenated. When an Al_2O_3 substrate was used, the relationship was MgH_2(110)[001] //

Mg(001)[100]. However, when a $LiGaO_2$ substrate was used, the relationship was MgH_2(200)[001] // Mg(110)[-111].

3.3 Structural model for the phase transformation: MgH_2 to Mg

Magnesium has an hcp structure with the atom stacking sequence of ABABAB.... Figure 4 (a) shows an image for the hcp stacking and Figure 4 (b) shows the atomic arrangement of MgH_2 and Mg viewed from the [110] and [0001] directions, respectively. Figures 4 (c) and (d) show a hexagonal unit cell for Mg and a analogous hcp unit cell for MgH_2 viewed from the [110] direction. For the analogous hcp unit cell of MgH_2, we calculate the cell parameters: a' = c = 3.01 Å, b' = 3.52 Å = 0.5 * $(a^2 + b^2 + c^2)^{1/2}$, and c' = 6.36 Å = 2 $d_{(110)}$ = $(a^2 + b^2)^{1/2}$. Next, we schematically show how MgH_2 transforms to Mg during dehydrogenation. As shown in Figures 4 (c) and (d), first, on the two layers of A, the value of a' for MgH_2 (3.01 Å) prolongs to Mg for a = 3.21 Å, and b' of MgH_2 (3.52 Å) shortens to Mg for b = 3.21 Å; at the same time, the angle of 64.7° shrinks to fit 60°. Along the c'-axis (c' = 6.36 Å), the two layers of A move toward each other to form Mg with c = 5.21 Å. Finally, on layer B, the atom from the (1/2, 1, 1/2) site of analogous hcp-MgH_2 will move to (1/3, 2/3, 1/2) of Mg. This scheme, presented in Figure 4, shows the movement of the Mg atoms of MgH_2 after losing hydrogen during the decomposition. Conversely, in the hydrogenation process, we believe that the Mg atoms move in the opposite directions for accepting hydrogen.

3.4 CONCLUSIONS

We investigated the phase transformation of MgH_2 to Mg by in situ (high-resolution) transmission electron microscopy using a sample of MgH_2 single-crystal nanofibers prepared by hydriding chemical vapor deposition. An electron beam induced the decomposition of MgH_2 to Mg. The results indicated the orientation relationship between MgH_2 and Mg during the phase change was one of the zone axis of MgH_2 <110> parallel to Mg [0001] zone axis, or one of the plane {110} of MgH_2 parallel to the basal plane of Mg (0001). On the basis of these results, we proposed a structure model for the phase transformation of MgH_2 to Mg.

Acknowledgements

The authors would like to thank Mr. G. Saito and Mr. K. Ohkubo for their technical support on TEM observation.

REFERENCES

[1] Jain IP, Lal C and Jain A. Hydrogen storage in Mg: A most promising material. International Journal of Hydrogen Energy 2010; **35**(10): p. 5133-5144.

[2] Sakintuna B, Lamari-Darkrim F and Hirscher M. Metal hydride materials for solid hydrogen storage: A review. International Journal of Hydrogen Energy 2007; **32**(9): p. 1121-1140.

[3] Garroni S, Milanese C, Girella A, Marini A, Mulas G, Menéndez E, Pistidda C, Dornheim M, Suriñach S and Baró MD. Sorption properties of $NaBH_4/MH_2$ (M = Mg, Ti) powder systems. International Journal of Hydrogen Energy 2010; **35**(11): p. 5434-5441.

[4] Kalisvaart WP, Harrower CT, Haagsma J, Zahiri B, Luber EJ, Ophus C, Poirier E, Fritzsche H and Mitlin D. Hydrogen storage in binary and ternary Mg-based alloys: A comprehensive experimental study. International Journal of Hydrogen Energy 2010; **35**(5): p. 2091-2103.

[5] Varin RA, Czujko T and Wronski Z. Particle size, grain size and gamma-MgH_2 effects on the desorption properties of nanocrystalline commercial magnesium hydride processed by controlled mechanical milling. Nanotechnology 2006; **17**(15): p. 3856-3865.

[6] Qu J, Wang Y, Xie L, Zheng J, Liu Y and Li X. Hydrogen absorption-desorption, optical transmission properties and annealing effect of Mg thin films prepared by magnetron sputtering. International Journal of Hydrogen Energy 2009; **34**(4): p. 1910-1915.

[7] Li WY, Li CS, Ma H and Chen J. Magnesium nanowires: Enhanced kinetics for hydrogen absorption and desorption. Journal of the American Chemical Society 2007; **129**(21): p. 6710-6711.

[8] Zhu C, Hayashi H, Saita I and Akiyama T. Direct synthesis of MgH_2 nanofibers at different hydrogen pressures. International Journal of Hydrogen Energy 2009; **34**(17): p. 7283-7290.

[9] Saita I, Toshima T, Tanda S and Akiyama T. Hydriding chemical vapor deposition of metal hydride nano-fibers. Materials Transactions 2006; **47**(3): p. 931-934.

[10] Zhu C, Hosokai S, Matsumoto I and Akiyama T. Shape-Controlled Growth of MgH_2/Mg Nano/Microstructures Via Hydriding Chemical Vapor Deposition. Crystal Growth & Design 2010; **10**(12): p. 5123-5128.

[11] Saita I, Toshima T, Tanda S and Akiyama T. Hydrogen storage property of MgH_2 synthesized by hydriding chemical vapor deposition. Journal of Alloys and Compounds 2007; **446-447**: p. 80-83.

[12] Horst E. Friedrich, Barry L. Mordike. Magnesium Technology. Springer - Verlag Berlin Heidelberg; 2006

[13] Paik B, Jones IP, Walton A, Mann V, Book D and Harris IR. $MgH_2 \rightarrow$ Mg phase transformation driven by a high-energy beam: An in situ transmission electron microscopy study. Philosophical Magazine Letters 2010; **90**(1): p. 1-7.

[14] Bokhonov B, Ivanov E and Boldyrev V. A study of the electron-beam-induced decompostion of magnesium hydride single-crystal. Materials Letters 1987; **5**(5-6): p. 218-221.

[15] Schober T. The magnesium-hydrogen system: Transmission electron microscopy. Metallurgical and Materials Transactions A 1981; **12**(6): p. 951-957.

[16] Kelekar R, Giffard H, Kelly ST and Clemens BM. Formation and dissociation of MgH_2 in epitaxial Mg thin films. Journal of Applied Physics 2007; **101**(11): p. 114311:1-7.

Table 1. Comparison of the orientation relationship between MgH_2 and Mg during phase transformation, derived by different researches.

Materials	*Preparation method*	*Observation method*	*Orientation relationship*	*Ref.*
HCVD MgH_2 nanofibers	MgH_2 Nanofibers prepared by hydriding chemical vapor deposition (HCVD)	(HR)TEM	(110)MgH_2//(0001)Mg	This study
MgH_2 powder (purity 95%)	Commercial product	TEM (200 kV)	[001]MgH_2//[-2110]Mg (-110)MgH_2//(0001)Mg	Paik B. et al. [13]
MgH_2 whisker	MgH_2 whiskers formed on the surface of Mg spheres hydrided at 630 K and 1.6 MPa	TEM	(110)MgH_2//(0001)Mg	Bokhonov B. [14]
MgH_2 disc	Mg discs hydrided at 270 ˚C and $5*10^6$Pa	TEM (120 kV)	[001]MgH_2//[-1-120]Mg (100)MgH_2//(0001)Mg	Schober T. [15]
Epitaxial Mg (001) thin films	Mg thin film formed on (001) Al_2O_3 substrate, then hydrided at 373 K and 0.6 MPa	XRD	[001]MgH_2//[100]Mg (110)MgH_2//(001)Mg	Kelekar R. [16]
Epitaxial Mg (110) thin films	Mg thin film formed on (320) $LiGaO_2$ substrate, then hydrided at 373 K and 0.6 MPa	XRD	[001]MgH_2//[-111]Mg (200)MgH_2//(110)Mg	Kelekar R. [16]

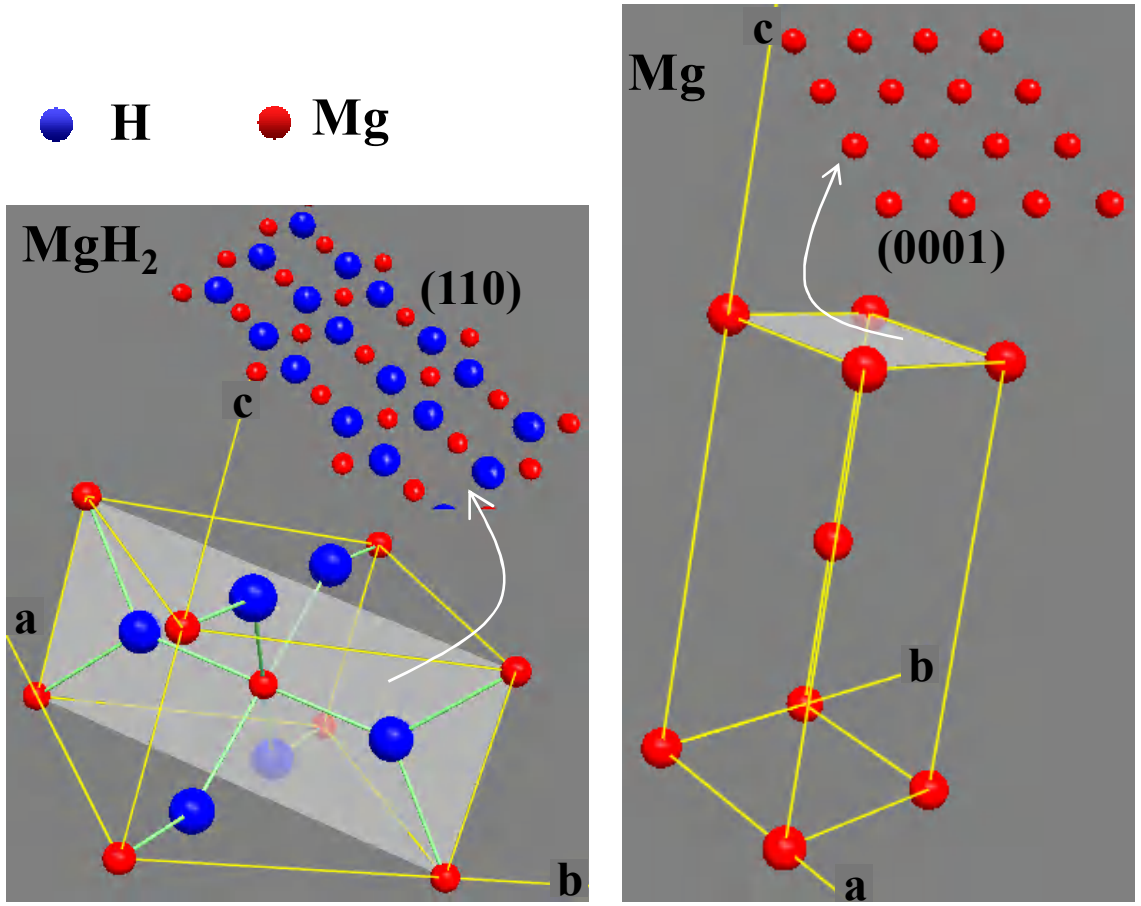

Figure 1. Unit cells of MgH_2 and Mg. Cell parameters for MgH_2 are a = b = 4.50 Å, c = 3.01 Å; cell parameters for Mg are a = b = 3.21 Å, c = 5.21 Å. Insets show the atomic arrangement on MgH_2 (110) and Mg (0001), respectively.

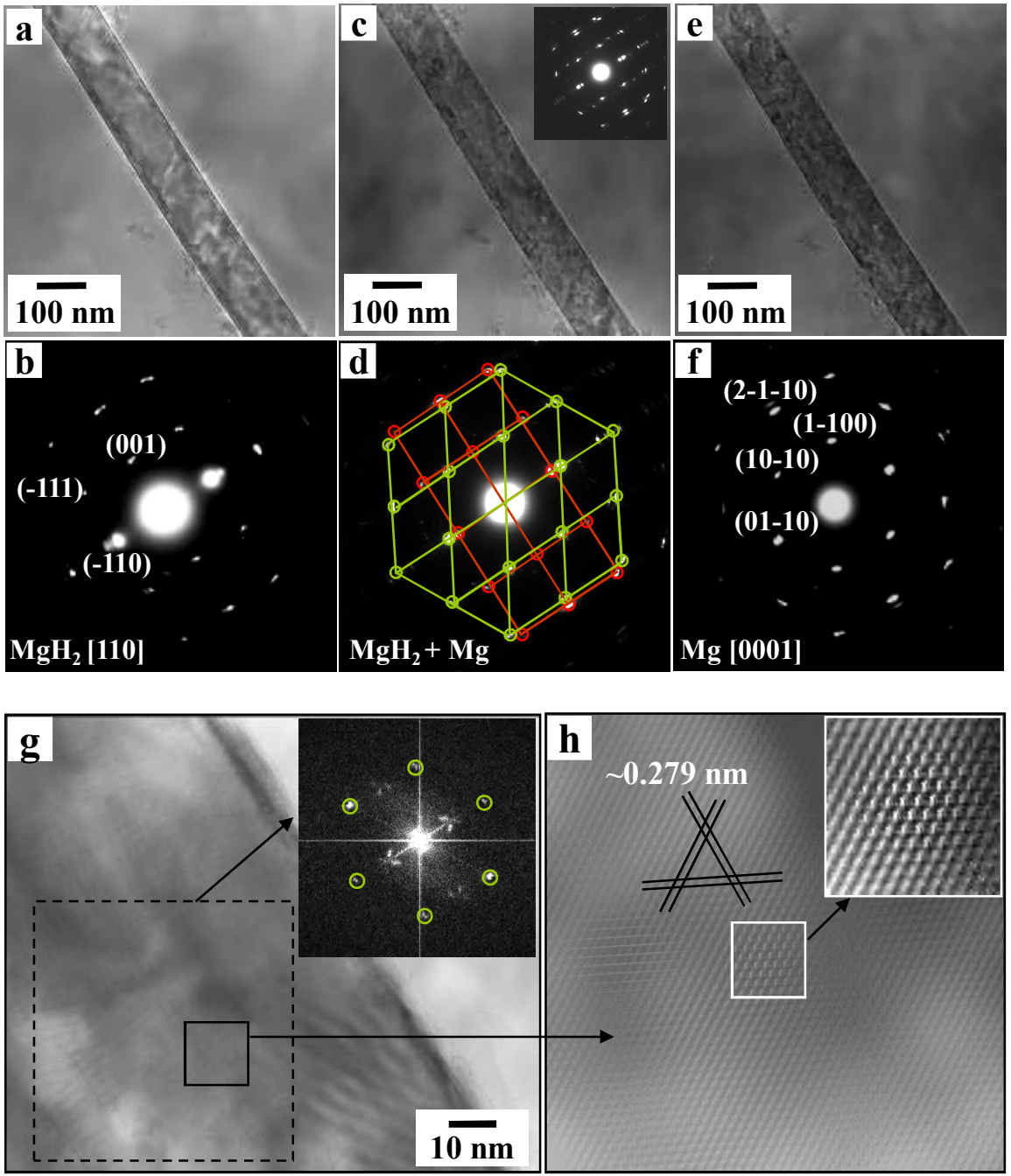
a
100 nm
c
100 nm
e
100 nm
b
(001)
(-111)
(-110)
MgH2 [110]
d
MgH2 + Mg
f
(2-1-10)
(1-100)
(10-10)
(01-10)
Mg [0001]
g
10 nm
h
~0.279 nm

Figure 2. A sequence of images (a, c and e) and SAED patterns (b, d and f) of an MgH_2 nanofiber at different stages of decomposition induced by an electron beam. (a, b) single phase of MgH_2; (c, d) both phases of MgH_2 and Mg; (e, f) strong reflection of Mg. (g) HRTEM image of the decomposed nanofiber after (e) ; the inset is the digital diffractogram based on Fast Fourier Transform (FFT) from the selected dash line area. (h) is the simulated lattice image obtained from the digital diffractogram in (g) showing Mg planes of {10-10}. Red cycles represent the diffraction spots of MgH_2 and the green ones are Mg.

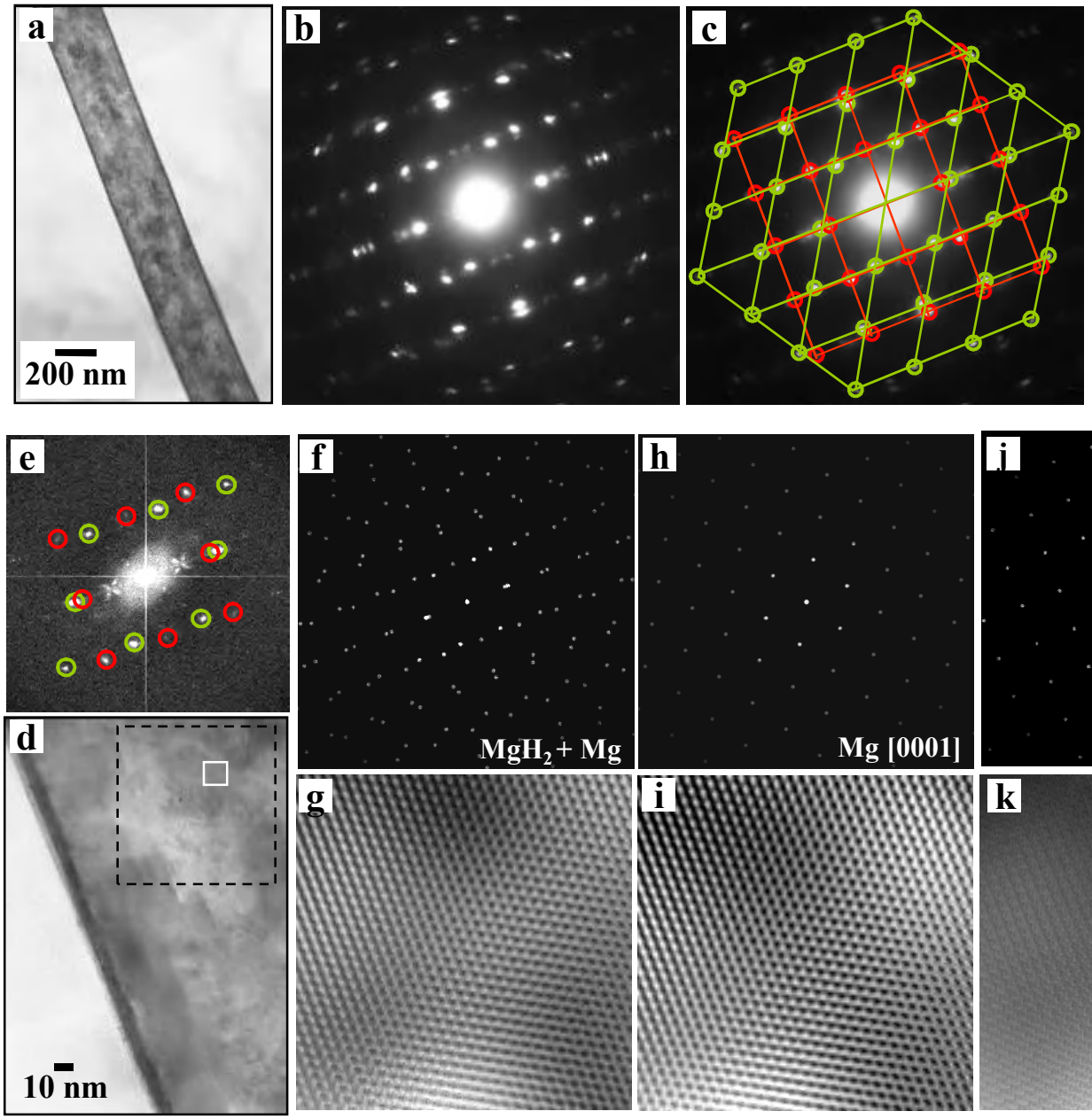
a
200 nm
b
c
e
f
MgH2 + Mg
h
Mg [0001]
i
MgH2 [110]
d
10 nm
g
i
k

Figure 3. Typical (high resolution) TEM images (a, d) and SAED pattern (b and c, c is the same pattern of b) showing both phases of MgH_2 and Mg during decomposition. (e) is the digital diffractogram based on Fast Fourier Transform (FFT) from the selected dash line area in (d); this pattern shows both phases of MgH_2 and Mg corresponding to that in (b, c). (f, g) are the simulated diffraction pattern and lattice image showing both phases of MgH_2 and Mg obtained from the FFT digital diffractogram. (h, i) are the simulated diffraction pattern and lattice image of Mg by masking the diffraction of MgH_2 in (e). (j, k) are the simulated diffraction pattern and lattice image of MgH_2 by masking the diffraction of Mg in (e). Red cycles represent the diffraction spots of MgH_2 and the green ones are Mg.

A

B

(a).

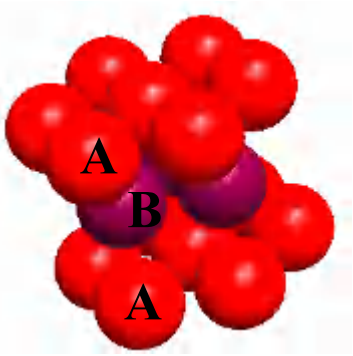
A
B
A

(b).

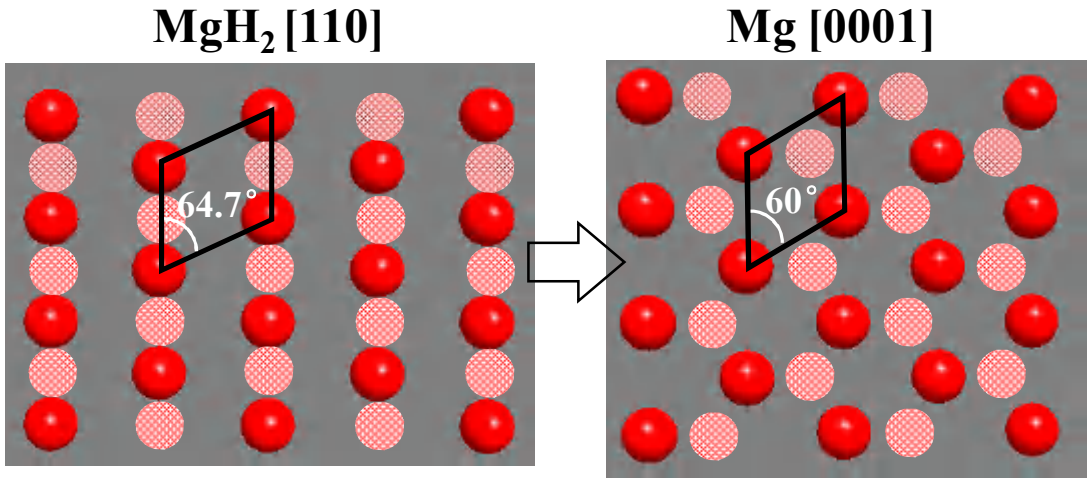
MgH2 [110]
Mg [0001]
64.7°
60°

(c).

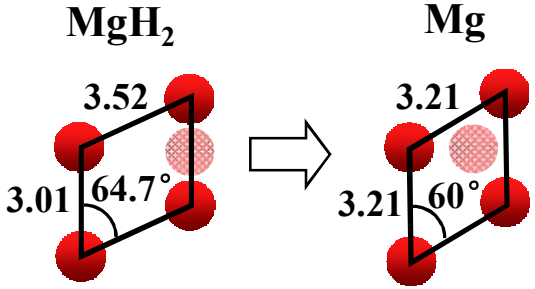
MgH2
Mg
3.52
3.01
64.7°
3.21
3.21
60°

(d).

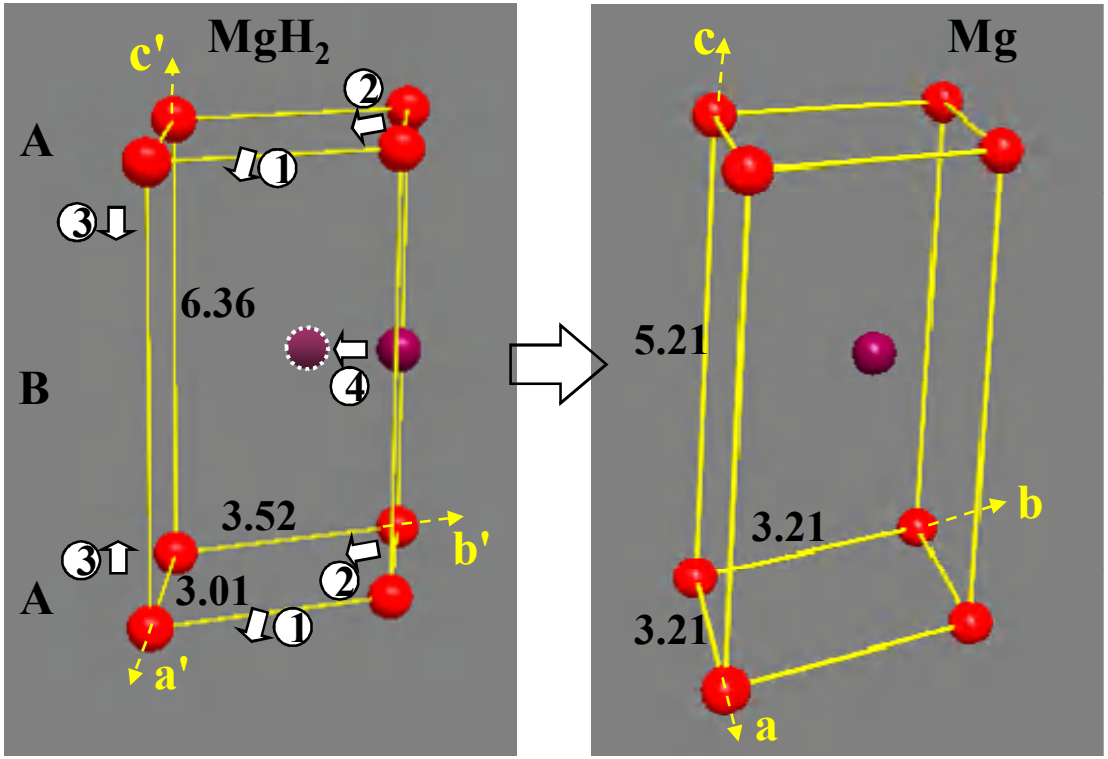
MgH2
Mg
c'
c
A
B
A
1
2
3
4
6.36
3.52
3.01
5.21
3.21
3.21
a'
b'
a
b

Figure 4. (a). Image for the hcp stacking, ABABAB…

(b). Atomic arrays of MgH_2 and Mg from [110] and [0001] view, respectively.

(c) and (d). The hexagonal unit cell for Mg and the analogous hcp unit cell for MgH_2 viewed from [110] direction, the H atom in MgH_2 is neglected, (c) is the projection view down MgH_2[110] and Mg[0001], (d) is the perspective view.

For the analogous hcp unit cell of MgH_2, $a' = c = 3.01$, $b' = 3.52 = 0.5 * (a^2 + b^2 + c^2)^{1/2}$, $c' = 6.36 = 2\ d_{(110)} = (a^2 + b^2)^{1/2}$. For Mg, $a = b = 3.21$, $c = 5.21$. All distances are expressed in Å.